Journal of Clinical and Translational Hepatology **2025** vol. 13(5) | 409–417
DOI: 10.14218/JCTH.2024.00440

Original Article

Inhibition of Cyclooxygenase-2 Upregulates the Nuclear Factor Erythroid 2-related Factor 2 Signaling Pathway to Mitigate Hepatocyte Ferroptosis in Chronic Liver Injury

Zhu Yang[1,2#], Yang Tai[1,2#], Tian Lan[1,2], Chong Zhao[2], Jin-Hang Gao[1,2], Cheng-Wei Tang[1,2*] and Huan Tong[1,2*]

[1]*Department of Gastroenterology and Hepatology, West China Hospital, Sichuan University, Chengdu, Sichuan, China;* [2]*Lab of Gastroenterology and Hepatology, West China Hospital, Sichuan University, Chengdu, Sichuan, China*

Received: November 23, 2024 | **Revised:** January 18, 2025 | **Accepted:** February 18, 2025 | **Published online:** March 03, 2025

Abstract

Background and Aims: Ferroptosis plays an essential role in chronic liver diseases, and cyclooxygenase-2 (COX-2) affects liver fibrosis through multiple mechanisms. However, research on COX-2 regulation of ferroptosis in chronic liver injury remains limited. This study aimed to investigate whether and how COX-2 regulates ferroptosis in chronic liver injury. ***Methods:*** *In vivo*, a thioacetamide (TAA)-induced chronic liver injury model, characterized by significant liver lipid peroxidation and oxidative stress, was used. *COX-2*$^{+/+}$ and *COX-2*$^{-/-}$ mice were treated with TAA or normal saline. *In vitro*, primary mouse hepatocytes were isolated and treated with dimethyl sulfoxide (DMSO), erastin+DMSO, etoricoxib+erastin+DMSO, and tBHQ+erastin+DMSO. Mitochondrial morphology, iron metabolism, lipid peroxidation, and oxidative stress were assessed to verify ferroptosis. The nuclear factor erythroid 2-related factor 2 (Nrf2) signaling pathway was measured to investigate the relationship between COX-2 and ferroptosis. ***Results:*** TAA-treated *COX-2*$^{-/-}$ mice presented milder liver fibrosis, whereas TAA-treated *COX-2*$^{-/-}$ mice livers and etoricoxib+erastin+DMSO-treated primary hepatocytes exhibited alleviated mitochondrial damage compared with TAA-treated *COX-2*$^{+/+}$ littermates and erastin+DMSO-treated primary hepatocytes, respectively. The knockout of COX-2 decreased ferrous ion concentration ($p < 0.01$) and mitigated lipid peroxidation in TAA-treated livers ($p < 0.05$). Furthermore, both COX-2 knockout and etoricoxib restored reduced glutathione ($p < 0.05$) and glutathione peroxidase 4 ($p < 0.05$), while decreasing malondialdehyde levels ($p < 0.05$). Additionally, COX-2 inhibition upregulated Nrf2, which helped alleviate erastin+DMSO-induced ferroptosis ($p < 0.01$). ***Conclusions:*** Ferroptosis contributes to the progression of chronic liver injury. Inhibition of COX-2 upregulates Nrf2, mitigating hepatocyte ferroptosis in chronic liver injury.

Keywords: Cyclooxygenase-2; Nuclear factor erythroid 2-related factor 2; Ferroptosis; Lipid peroxidation; Oxidative stress; Hepatocytes; Chronic liver injury.
[#]Contributed equally to this work.
[*]**Correspondence to**: Huan Tong and Cheng-Wei Tang, Department of Gastroenterology and Hepatology, West China Hospital, Sichuan University, No 37, Guo Xue Xiang, Chengdu, Sichuan 610041, China. ORCID: https://orcid.org/0000-0002-2874-5675 (HT) and https:/orcid.org/0000-0002-2289-8240 (CWT). Tel: +86-28-85164011, E-mail: doctortonghuan@163.com (HT) and shcqcdmed@163.com (CWT).

Citation of this article: Yang Z, Tai Y, Lan T, Zhao C, Gao JH, Tang CW, *et al*. Inhibition of Cyclooxygenase-2 Upregulates the Nuclear Factor Erythroid 2-related Factor 2 Signaling Pathway to Mitigate Hepatocyte Ferroptosis in Chronic Liver Injury. J Clin Transl Hepatol 2025;13(5):409–417. doi: 10.14218/JCTH.2024.00440.

Introduction

Liver cirrhosis poses a substantial disease burden worldwide due to its increased probability of developing serious complications, such as massive variceal bleeding, refractory ascites, and hepatorenal syndrome.[1] Liver cirrhosis is the end-stage of progressive fibrosis caused by persistent chronic liver injury. Chronic injuries lead to hepatocyte death, which subsequently initiates and exacerbates liver fibrosis.[2] Unlike other types of cell death, such as apoptosis, necrosis, and autophagy, ferroptosis is an iron-dependent form of regulated cell death characterized by impaired mitochondrial morphology, iron overload, disturbed lipid peroxidation, and excessive oxidative stress.[3] Ferroptosis has been implicated in several liver diseases, such as drug-induced liver injury, ischemia-reperfusion injury, chronic liver disease, and hepatocellular carcinoma.[4]

Cyclooxygenase (COX) is a key rate-limiting enzyme in the conversion of arachidonic acid (AA) to prostaglandins (PTGS), thromboxane, and prostacyclin.[5] There are three isomers of COX: COX-1, COX-2, and COX-3.[6] Among these isomers, COX-2 is widely believed to participate in inflammation and tumorigenesis.[7,8] Furthermore, our previous studies have revealed that COX-2 is involved in and regulates the progression of liver fibrosis/cirrhosis via various mechanisms.[9–11] However, whether COX-2 regulates ferroptosis to impact liver fibrosis has yet to be thoroughly investigated.

Many transcription factors, including nuclear factor erythroid 2-related factor 2 (Nrf2), regulate ferroptosis.[12,13] Nrf2 is pivotal for regulating various pathophysiological processes, such as cellular redox status, detoxification, and anti-inflammatory responses.[14] Considering that both Nrf2 and COX-2 regulate inflammation, Nrf2 may act as a link between COX-2 and ferroptosis in the context of chronic liver injury. Therefore, this study aimed to investigate whether COX-2

regulates ferroptosis via the Nrf2 signaling pathway during the progression of chronic liver injury.

Methods

Animal model

The animal experiments were approved by the Animal Use and Nursing Committee of West China Hospital of Sichuan University. Wild-type, *Ella*^{Cre}, and *COX-2*$^{flox/flox}$ C57BL/6 mice were purchased from GemPharmatech (Nanjing, China) for this study. All the mice were maintained under constant temperature and humidity with standard 12-h light-dark cycles and had free access to diet in the experimental animal center of Sichuan University (Chengdu, China). *Ella*^{Cre} mice were crossed with *COX-2*$^{flox/flox}$ mice to generate conventional *COX-2* knockout mice (*COX-2*$^{-/-}$) and littermate controls (*COX-2*$^{+/+}$).[15] Age-matched male mice (six to eight weeks old, weighting 20–25 g) were selected for further experiments. Thioacetamide (TAA), which induces lipid peroxidation and oxidative stress—two components of ferroptosis—was employed to establish a chronic liver injury model in this study.[16] Mice were randomly allocated to different groups, with six mice in each group. *COX-2*$^{+/+}$ mice in the control (CO) normal saline (NS) group and *COX-2*$^{-/-}$ mice in the knockout (KO) NS group were injected intraperitoneally with NS at a dosage of 0.2 mL/d every three days for eight weeks. *COX-2*$^{+/+}$ mice in the CO TAA group and *COX-2*$^{-/-}$ mice in the KO TAA group were injected intraperitoneally with 4% thioacetamide (TAA, Sigma-Aldrich, USA) dissolved in NS at a dosage of 200 mg/kg every three days for eight weeks.[15] Mice were anesthetized with sodium pentobarbital and sacrificed three days after the last intraperitoneal injection to harvest liver samples. Liver samples were fixed for light or transmission electron microscopy (TEM) evaluation or stored at −80°C for quantitative real-time polymerase chain reaction (qRT-PCR), Western blot, lipid metabolomics, and measurements of ferrous ions, hepcidin, glutathione (GSH), and malondialdehyde (MDA).

Isolation and treatments of primary mouse hepatocytes

Primary mouse hepatocytes were isolated from eight-to-twelve-week-old male C57BL/6 mice using the two-step collagenase perfusion method, as previously described.[17] Briefly, hepatocytes were isolated by digestion with type II collagenase (17101015, Gibco, Grand Island, USA) and then separated by Percoll (P1644, Sigma-Aldrich, USA) for centrifugation. The isolated hepatocytes were cultured in serum-free medium (DMEM-F12, Gibco™) for 12 h, and then treated with 0.1% dimethyl sulfoxide (DMSO) (Solarbio, Beijing, China), erastin (20 μM, ferroptosis inducer, S7242, Selleck, Shanghai, China) + DMSO, etoricoxib (10 μM, selective COX-2 inhibitor with the best affinity to COX-2, HY-15321, MedChem Express, Shanghai, China) + erastin (20 μM) + DMSO, and tBHQ (50 μM, Nrf2 agonist, HY-100489, MedChem Express, Shanghai, China) + erastin (20 μM) + DMSO for 8 h. Erastin, etoricoxib, and tBHQ were dissolved in DMSO. After interventions, primary hepatocytes were fixed on coverslips for immunofluorescence staining, or scraped from culture dishes and fixed for TEM evaluation, or scraped and stored at −80°C for qRT-PCR, Western blot, and GSH and prostaglandin E2 (PGE2) measurements.

Light microscopy and TEM

Liver specimens from mice were fixed in 4% formalin, embedded in paraffin, and sectioned into 4-μm-thick slices. Hematoxylin and eosin (HE) and Sirius red staining were used for histological evaluation and assessment of collagen deposition, respectively.[9] TEM (JEM1200EX, JEOL, Japan) was performed to evaluate changes in mitochondrial morphology following a standard protocol.[18] In brief, liver tissues and primary mouse hepatocytes were collected, fixed in 4% glutaraldehyde (Solarbio, Beijing, China) for 2 h, and then fixed in 1% osmium tetroxide for 1 h at 4°C. The samples were dehydrated, embedded in epoxy resin, and sectioned into 70-nm-thick slices for microscopic examination. These slices were stained with 5% uranyl acetate and examined under a TEM. All slides were observed and evaluated by two technicians independently, who were blinded to the sample identification information. Their conclusions were compared, and if discrepancies were found, a third technician was included to make a final determination.

Immunofluorescence staining

Primary mouse hepatocytes were cultured on coverslips at the bottom of 24-well plates. After treatment, the samples were fixed with 4% paraformaldehyde, rinsed with phosphate buffer solution, and then permeabilized with 0.1% Triton-X-100.[19] The samples were blocked with donkey serum and incubated with a primary antibody against mouse glutathione peroxidase 4 (GPX4) (dilution: 1:200, 67763-1-Ig, Proteintech, Wuhan, China) and secondary antibodies. The slides were coverslipped with anti-fading medium containing 4′, 6-diamidino-2-phenylindole and scanned using a fluorescence microscope.

Ferrous ion, hepcidin, GSH, MDA, and PGE2 measurements

Liver tissues were processed in NS to create tissue homogenates in an ice-water bath and then centrifuged. The supernatants were collected for the measurement of various indicators. Primary mouse hepatocytes were collected through ultrasonication with phosphate buffer solution in an ice-water bath after the intervention, and the resulting centrifugal supernatants were gathered. Concentrations of ferrous ion, hepcidin, GSH, MDA, and PGE2 were measured according to the manufacturer's instructions (Jiancheng, Nanjing).[20] Ferrous ion was determined using a colorimetric assay kit (A039-2-1, Jiancheng, Nanjing), where the centrifugal supernatants were mixed with chromogenic reagents for colorimetric detection at 520 nm using a spectrophotometer. Hepcidin and PGE2 were measured using enzyme-linked immunosorbent assay kits (Hepcidin: H252, Jiancheng, Nanjing; PGE2: H099-1-2, Jiancheng, Nanjing). Briefly, processed liver tissues and primary hepatocytes were added to enzyme pre-coated wells with antibodies, and recognition antigens were incubated for 30 m at 37°C to form immune complexes, which were then detected at 450 nm. GSH was measured with a spectrophotometric kit (A006-1-1, Jiancheng, Nanjing), quantitatively determined at 420 nm. MDA was measured using a thiobarbituric acid (TBA) assay kit (A003-1-2, Jiancheng, Nanjing), where TBA reagents were added to the centrifugal supernatants to generate the MDA-TBA complex, detected at 532 nm.

Western blot

Proteins were extracted from frozen liver tissues and primary mouse hepatocytes using a protein extraction kit (KGP2100, KeyGEN BioTECH, Jiangsu, China). Protein concentrations were measured using a bicinchoninic acid assay kit (P0010, Beyotime Biotechnology, Shanghai, China). Proteins (50 μg from liver tissues, 30 μg from hepatocytes) were separated by 10% sodium dodecyl sulfate-polyacrylamide gel

Table 1. Primer sequences

Gene	Forword	Reverse
β-actin	5′-AAGGCCAACCGTGAAAAGAT-3′	5′-GTGGTACGACCAGAGGCATAC-3′
Gpx4	5′-GCAGGAGCCAGGAAGTAATC-3′	5′-GGCTGGACTTTCATCCATTT-3′
Tfr	5′-AAGCCAGATCAGCATTCTCT-3′	5′-CGGCATTTTCTTCT CATCT-3′
Fpn	5′-TTGCAGGAGTCATTGCTGCTA-3′	5′-TGGAGTTCTGCACACCATT-3′
Ptgs2	5′-ATTCCAAACCAGCAGACTCATA-3′	5′-CTTGAGTTTGAAGTGGTAACCG-3′
Slc7a11	5′-AACCAACAAGCAGGTGGTTGA-3′	5′-CCTTGTAGATGTCCACAGCCAGAGT-3′

Gpx4, glutathione peroxidase 4; Tfr, transferrin; Fpn, ferroportin; Ptgs2, prostaglandin 2.

electrophoresis and transferred to polyvinylidene difluoride membranes. The membranes were blocked in 5% defatted milk in TBST and incubated with specific primary antibodies overnight at 4°C,[10] including mouse GPX4 (dilution: 1:1,000, 67763-1-Ig, Proteintech, Wuhan, China) and rabbit NRF2 (dilution: 1:2,000, 16396-1-Ap, Proteintech, Wuhan, China). After binding with secondary antibodies (dilution: 1:20,000, ZB-2301, ZB-2305, Santa Cruz, USA), the target protein blots were visualized using an enhanced chemiluminescence detection kit (P0018AM, Beyotime Biotechnology, Shanghai, China) and exposed on a chemiluminescence imaging system (ChemiScope6100, Clinc, Shenzhen, China).

qRT-PCR

Total RNA was extracted from liver tissues and primary mouse hepatocytes using TRIzol (RE-03011, RE-03113, FOREGENE, Chengdu, China). RNA was reverse-transcribed into cDNA using a first-strand cDNA kit (K1691, Thermo Scientific, Shanghai, China). qRT-PCR was conducted using SYBR Green probes (Thermo Scientific, Shanghai, China).[21] The sequences of primers used in this study are listed in Table 1. The results were normalized to β-actin using the $2^{-\Delta\Delta Ct}$ method.

Lipid metabolomics

Liver tissues were pretreated, and hydrophilic or hydrophobic metabolites were extracted. Liquid chromatography-tandem mass spectrometry (MS/MS) was used to detect lipid metabolites. Ultraperformance liquid chromatography (UPLC, ExionLC AD system, SCIEX, Shanghai, China) and tandem mass spectrometry (MS/MS, QTRAP® System, SCIEX, Shanghai, China) were applied for lipid information collection.[22] Based on the MetWare database, secondary data were analyzed qualitatively and quantitatively according to the retention time, precursor ions, and product ions of the detected substances.

Statistical analysis

All quantitative variables were expressed as mean ± SD and analyzed using SPSS 22.0 software (IBM, Inc., Chicago, IL, USA). One-way analysis of variance was applied for comparisons among multiple groups. Graphs were generated using GraphPad Prism 8.0 (GraphPad, Inc., La Jolla, CA, USA). A two-tailed *p*-value of <0.05 was considered statistically significant.

Results

COX-2 deteriorated hepatocyte morphology under both TAA and erastin treatments

Under intraperitoneal TAA challenge, the liver structure of *COX-2*$^{+/+}$ mice, as revealed by HE staining, underwent significant changes, characterized by inflammatory cell infiltration and fibrotic septa formation in the liver tissue. In contrast, liver inflammation and fibrosis were milder in TAA-treated *COX-2*$^{-/-}$ mice (Fig. 1A). The fibrotic area of the liver shrank by 63.1% in the KO TAA group compared to the CO TAA group (CO TAA *vs.* KO TAA: 6.5 ± 2.2 % *vs.* 2.4 ± 0.2 %, $p = 0.002$). These findings are consistent with our previous studies on the role of COX-2 in chronic liver injury.[15]

TEM revealed smaller and ruptured mitochondria, with fewer cristae in the livers of the CO TAA group compared to those in the CO NS group (Fig. 1A). Additionally, high-density substances were deposited in the hepatocyte mitochondria of the CO TAA group. These mitochondrial morphological changes are consistent with the characteristics of ferroptosis. However, the hepatocyte mitochondria of the KO TAA group did not show remarkable shifts compared to those in the CO TAA group. Furthermore, erastin induced ferroptosis in primary mouse hepatocytes, with smaller mitochondria and fewer cristae, whereas etoricoxib, a selective COX-2 inhibitor, partially reversed the mitochondrial abnormalities induced by erastin (Fig. 1B).

COX-2 affected iron metabolism in TAA-induced chronic liver injury

Given that COX-2 was involved in mitochondrial changes related to ferroptosis, iron metabolism was the next focus of this study. Under TAA challenge, ferrous ion levels were examined by a colorimetric assay, which revealed a two-fold increase from 0.22 ± 0.11 mg/gram protein in the CO NS group to 0.48 ± 0.12 mg/gram protein in the CO TAA group ($p = 0.017$) (Fig. 2A). In contrast, the ferrous ion level in the livers of the KO TAA group (0.18 ± 0.04 mg/gram protein) was only 37.5% of that in the CO TAA group ($p = 0.004$) (Fig. 2A). Several molecules are involved in maintaining iron homeostasis. Transferrin (Tfr) facilitates iron transport into cells, while ferroportin (Fpn) exports iron out of cells. Hepcidin interacts with and degrades Fpn to inhibit iron efflux.[23] In our study, although hepcidin, Tfr, and Fpn did not show significant differences between the different phenotypes of COX-2, these biomolecules still tended to be affected by COX-2, thereby altering iron metabolism (Fig. 2B–D).

COX-2 modulated lipid peroxidation and oxidative stress in TAA-induced chronic liver injury and erastin-induced hepatocyte ferroptosis

Lipid peroxidation is pivotal for initiating ferroptosis, and polyunsaturated fatty acids are the most susceptible lipids in peroxidation, such as arachidonic acid (AA, C20:4), adrenic acid (AdA, C22:4), linoleic acid (Lin, C18:2), and C22:6.[24] Furthermore, phosphatidylethanolamine, phosphatidylcholine, and phosphatidylserine have been previously reported

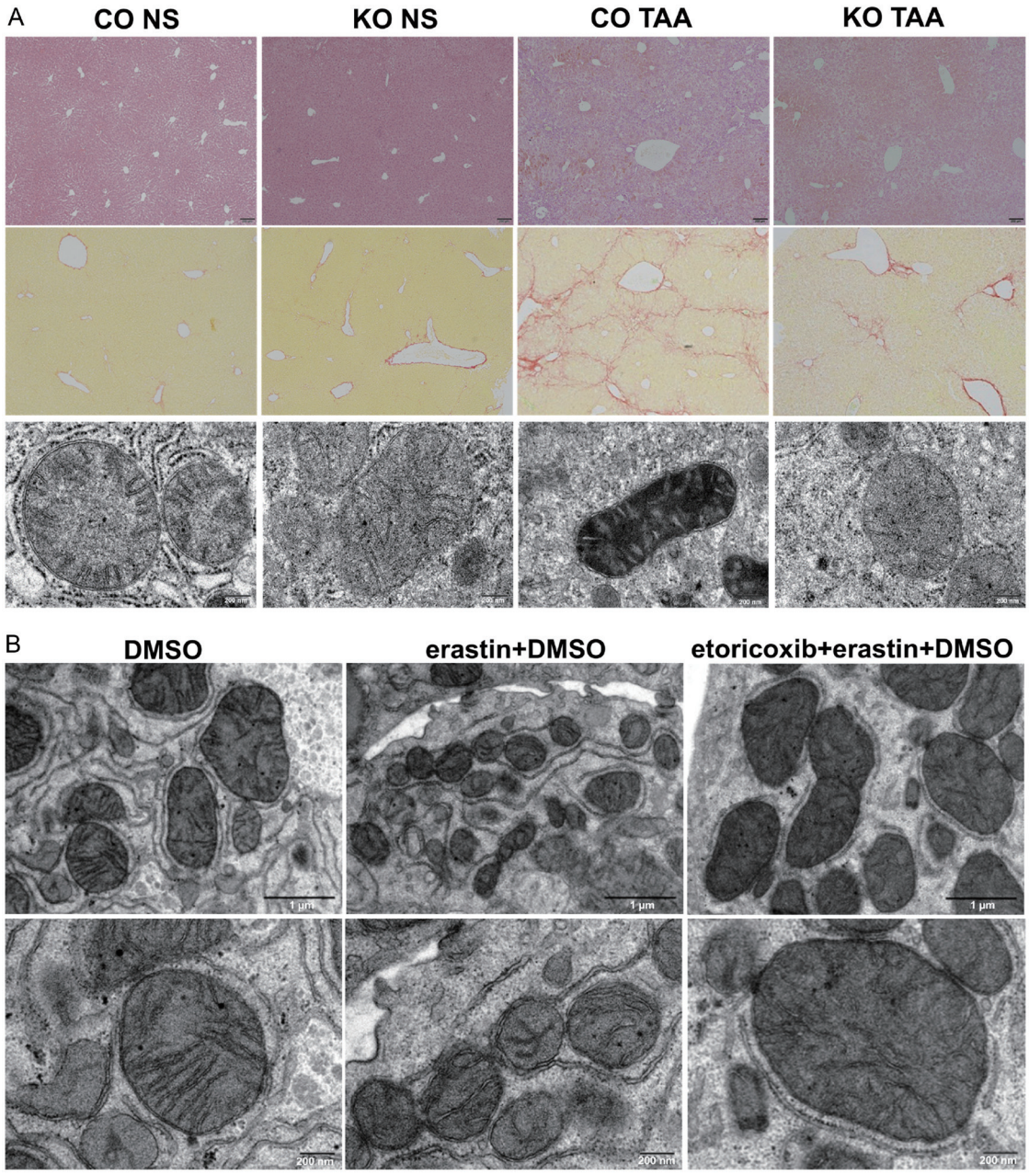

Fig. 1. Microscopic changes in mouse livers and primary mouse hepatocytes. (A) Liver specimens under light and electron microscopy. Liver tissues in the first and second rows were stained with hematoxylin-eosin and Sirius red, respectively (×100 magnification). Liver tissues in the third row show hepatocyte mitochondrial changes under transmission electron microscopy (×20,000 magnification, scale bar 200 nm) (n = 6 for each group). (B) Isolated primary hepatocytes under transmission electron microscopy (First row: ×4,000 magnification, scale bar 1 μm; second row: ×20,000 magnification, scale bar 200 nm) (n = 6 for each group). CO, control; KO, knockout; NS, normal saline; TAA, thioacetamide; DMSO, dimethyl sulfoxide.

as the most relevant phospholipids in ferroptosis.[25] Liquid chromatography–MS/MS-based lipidomic data from our study revealed that free fatty acids (FFAs) in the liver differed between the CO TAA and KO TAA groups, while similar levels of phosphatidylcholine, phosphatidylethanolamine, and phosphatidylserine were detected in these two groups (Fig. 3A–D). Specifically, AA, AdA, Lin, and FFA (C22:6) all decreased in the livers of the KO TAA group by 36.1%, 39.4%, 30.1%, and 37.4%, respectively [CO TAA *vs.* KO TAA: AA (11.34 ± 1.93) × 10^5 *vs.* (7.25 ± 1.31) × 10^5, p = 0.038; AdA (10.78 ± 1.64) ×10^6 *vs.* (6.53 ± 0.66) × 10^6, p = 0.014; Lin (1.55 ± 0.08) × 10^8 *vs.* (1.08 ± 0.09) × 10^8, p = 0.003; FFA (C22:6) (2.93 ± 0.17) × 10^7 *vs.* (1.83 ± 0.16) × 10^7, p = 0.001; Fig. 3E–H].

As a downstream event of lipid oxidation, oxidative stress fuels ferroptosis and contributes to cell damage. GPX4, together with GSH, plays a pivotal role in countering oxidative stress during ferroptosis. MDA, a metabolite of lipid peroxidation, reflects the intensity of lipid peroxidation and oxidative stress. In the CO TAA group, GSH and MDA levels,

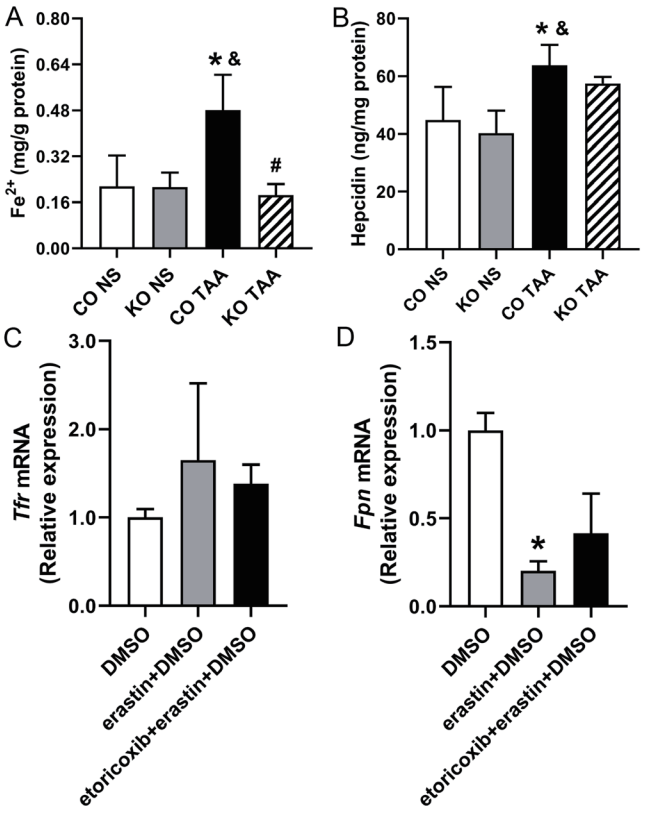

Fig. 2. Iron metabolism in mouse livers and primary mouse hepatocytes. (A, B) Ferrous ion and hepcidin concentrations in the liver (n = 6 for each group). (C, D) The mRNA expression levels of *Tfr* and *Fpn* in primary mouse hepatocytes (n = 6 for each group). (A, B) $p < 0.05$: **vs.* CO NS group; $^{\&}$*vs.* KO NS group; $^{\#}$*vs.* CO TAA group. (C, D) $p < 0.05$: **vs.* DMSO group; $^{\#}$*vs.* erastin + DMSO group. Tfr, transferrin; Fpn, ferroportin; CO, control; NS, normal saline; KO, knockout; TAA, thioacetamide; DMSO, dimethyl sulfoxide.

as determined by spectrophotometry, were significantly depleted in the liver, while GSH and MDA levels were restored in the liver of the KO TAA group (CO TAA *vs.* KO TAA: GSH, 2.24 ± 0.24 μmol/g protein *vs.* 3.63 ± 0.16 μmol/g protein, $p < 0.001$; MDA, 0.62 ± 0.26 nmol/mg protein *vs.* 0.39 ± 0.04 nmol/mg protein, $p = 0.015$) (Fig. 4A, B). The loss of COX-2 downregulated GPX4 in the liver after TAA treatment (CO TAA *vs.* KO TAA: 0.47 ± 0.26 *vs.* 1.23 ± 0.19, $p = 0.027$) (Fig. 4C). Regarding primary mouse hepatocytes treated with erastin, *Ptgs2* mRNA expression and PGE2 levels were higher than those in DMSO treatment (DMSO *vs.* erastin+DMSO: *Ptgs2* mRNA, 1.00 ± 0.06 *vs.* 2.75 ± 0.36, $p = 0.001$; PGE2, 37.01 ± 5.12 ng/L *vs.* 55.40 ± 6.60 ng/L, $p = 0.005$), while etoricoxib reversed these effects (erastin+DMSO *vs.* etoricoxib+erastin+DMSO: *Ptgs2* mRNA, 2.75 ± 0.36 *vs.* 1.91 ± 0.31, $p = 0.037$; PGE2, 55.40 ± 6.60 ng/L *vs.* 40.35 ± 6.49 ng/L, $p = 0.017$) (Fig. 4D, E). GSH decreased in the erastin+DMSO group, and etoricoxib reversed the GSH decrement induced by erastin (erastin+DMSO *vs.* etoricoxib+erastin+DMSO: 10.72 ± 0.91 μmol/g protein *vs.* 21.62 ± 4.02 μmol/g protein, $p = 0.002$) (Fig. 4F), which was even higher than that induced by DMSO treatment (13.46 ± 1.87 μmol/g protein). Etoricoxib also inhibited the production of MDA in primary mouse hepatocytes (erastin+DMSO *vs.* etoricoxib+erastin+DMSO: 1.05 ± 0.08 nmol/mg protein *vs.* 0.91 ± 0.08 nmol/mg protein, $p = 0.045$) (Fig. 4G), which was close to the results of the DMSO treatment (0.82 ± 0.09 nmol/mg protein). Slc7a11, a membrane transporter for GSH synthesis, was restored in the etoricoxib+erastin+DMSO group compared with the erastin+DMSO group (erastin+DMSO *vs.* etoricoxib+erastin+DMSO: 0.61 ± 0.07 *vs*. 3.13 ± 0.71, $p = 0.004$) (Fig. 4H). In addition, both GPX4 mRNA and protein levels were also recovered in the etoricoxib+erastin+DMSO group (erastin+DMSO *vs.* etoricoxib+erastin+DMSO: GPX4 mRNA, 0.65 ± 0.01 *vs*. 0.84 ± 0.06, $p = 0.004$; GPX4 protein, 0.45 ± 0.04 *vs*. 0.89 ± 0.24, $p = 0.034$) (Fig. 4I–K).

Inhibition of COX-2 upregulates the Nrf2 signaling pathway to attenuate ferroptosis

The aforementioned results suggested that COX-2 was implicated in ferroptosis. Since the Nrf2 signaling pathway is involved in antioxidation, it is important to explore whether this pathway plays a bridging role between COX-2 and ferroptosis. Data from primary mouse hepatocytes showed that the Nrf2 agonist tBHQ upregulated the Nrf2 signaling pathway to reverse the decline of GPX4 induced by erastin (erastin+DMSO *vs.* tBHQ+erastin+DMSO: Nrf2, 0.21 ± 0.02 *vs.* 0.55 ± 0.17, $p = 0.026$; GPX4, 0.61 ± 0.11 *vs.* 1.16 ± 0.25, $p = 0.025$) (Fig. 5A). These results also suggested that the inhibition of COX-2 by etoricoxib could upregulate the Nrf2 signaling pathway to ameliorate erastin-induced ferroptosis (erastin+DMSO *vs.* etoricoxib+erastin+DMSO: Nrf2 protein, 0.32 ± 0.08 *vs*. 0.85 ± 0.09, $p = 0.002$) (Fig. 5B).

Discussion

Ferroptosis, an alternative form of programmed cell death, is implicated in various disease processes, such as tissue injury, cancer, and neurodegenerative diseases.[26,27] In the chronic liver injury mice of this study, damaged mitochondria in hepatocytes and increased iron concentrations, along with enhanced lipid peroxidation and oxidative stress, suggest that chronically injured livers undergo ferroptosis. Ferroptosis is thought to play a dual role in liver fibrosis. On the one hand, ferroptosis regulates the autophagy signaling pathway in hepatic stellate cells to alleviate liver fibrosis.[28] On the other hand, ferroptosis promotes liver fibrosis in global and hepatocyte-specific gene-modified mice.[12,29,30] As the liver is home to various types of cells, with hepatocytes accounting for the majority (~80%),[31] ferroptosis in the large population of hepatocytes would be potent enough to outweigh ferroptosis in hepatic stellate cells, thus determining the fate of the liver. Our study also revealed that TAA-treated mouse livers underwent both ferroptosis and fibrosis. Liver fibrosis was mitigated when ferroptosis was simultaneously inhibited by global knockout or inhibition of COX-2, supporting the notion that ferroptosis of hepatocytes is detrimental to the progression of chronic liver disease.

COX-2 is a versatile protein involved in the pathogenesis of deteriorating liver fibrosis and cirrhosis. COX-2 induces hepatocyte–cholangiocyte transdifferentiation,[15] promotes hepatocyte apoptosis by inhibiting endoplasmic reticulum stress,[9] and inhibits the epithelial–mesenchymal transition of hepatocytes.[32] In this study, inhibition of COX-2 not only restored the damaged mitochondria in hepatocytes and reduced iron concentrations in TAA-treated liver tissue and erastin-treated primary mouse hepatocytes, but also decreased the levels of polyunsaturated fatty acids, including Lin, AA, AdA, and C22:6, and downregulated lipid peroxidation and oxidative stress. These findings indisputably suggest that COX-2 accelerates ferroptosis, influencing the progression of chronic liver disease. Other investigators have reported that COX-2 regulates ferroptosis in renal and cerebral conditions.[33–35] These

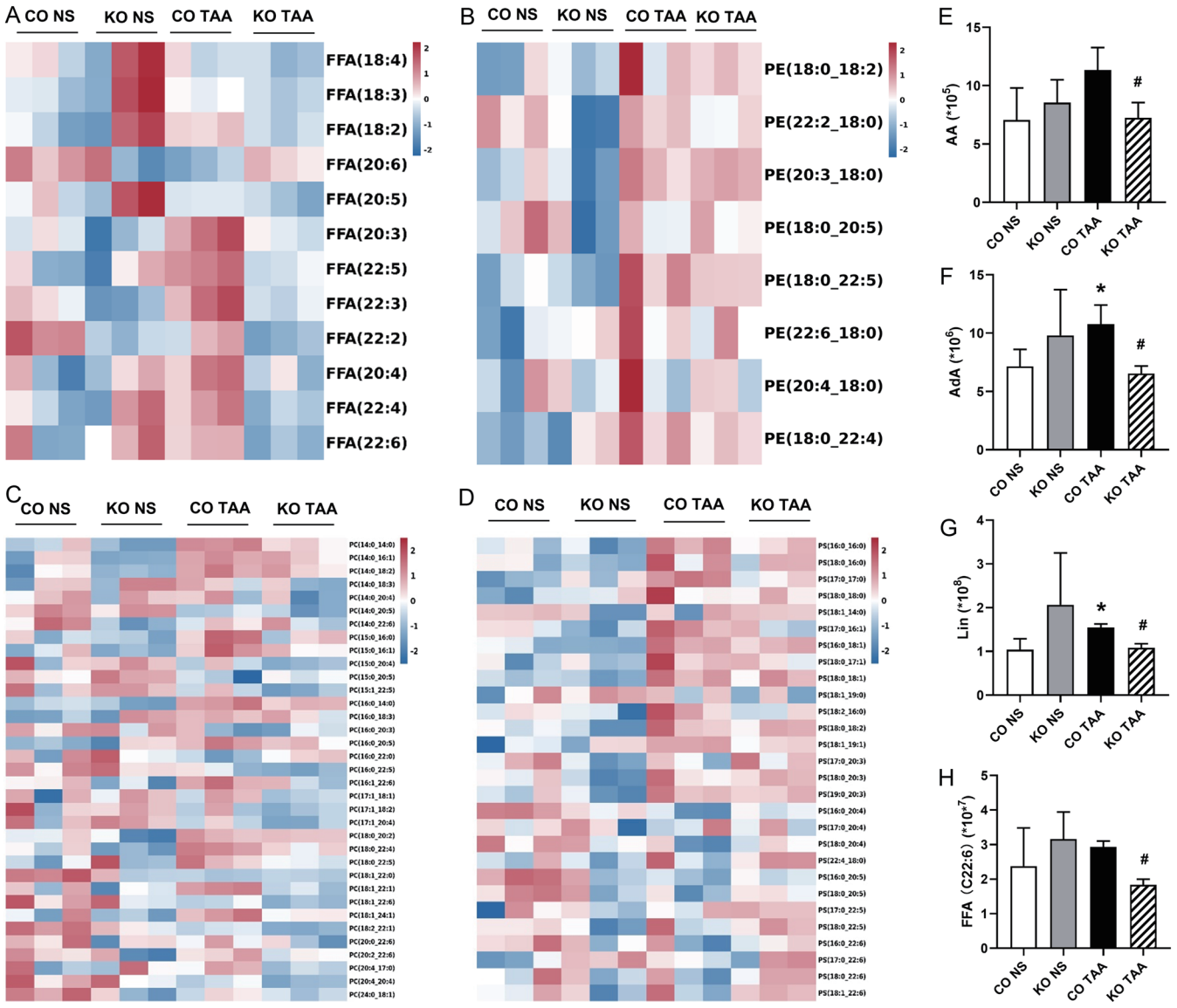

Fig. 3. Lipid metabolomics of mouse livers. (A–D) Heatmaps of FFAs (A), PE (B), PC (C), and PS (D) (n = 6 for each group). (E–H) Concentrations of AA (E), AdA (F), Lin (G), and FFA (C22:6) (H) (n = 6 for each group). $p < 0.05$: **vs.* CO NS group; #*vs.* CO TAA group. FFA, free fatty acid; PE, phosphatidylethanolamine; PC, phosphatidylcholine; PS, phosphatidylserine; AA, arachidonic acid; AdA, adrenic acid; Lin, linoleic acid; CO, control; NS, normal saline; KO, knockout; TAA, thioacetamide.

results share some similarities with our findings. In contrast, there is also a study suggesting that COX-2 is a downstream molecule of ferroptosis.[36] Yang *et al*. reported that erastin- or (1S, 3R)-RSL3-induced ferroptotic cell death was not affected by indomethacin, and that *PTGS2*, the gene encoding COX-2, is a downstream marker of ferroptosis.[36] However, our data revealed a different relationship between COX-2 and ferroptosis. Our findings indicated that inhibition of COX-2 activated the Nrf2 signaling pathway to relieve ferroptosis in the liver, positioning COX-2 upstream in the regulation of ferroptosis in liver fibrosis. There are two possible reasons for this distinction compared to the published work.[36] First, the BJeLR cells used by Yang *et al*. were derived from human skin and were engineered to express the catalytic subunits of human telomerase, SV40 large T and small T antigens, and an oncogenic allele of HRAS. In contrast, our study utilized mouse livers and primary mouse hepatocytes. Second, Yang *et al*. focused on malignancy, while we focused on chronic liver injury, which is a benign disease by nature. Additionally, the indomethacin used by Yang *et al*. is a non-selective COX inhibitor that can bind both COX-1 and COX-2 simultaneously to exert its pharmacological effects. In contrast, we employed COX-2 knockout mice and a selective COX-2 inhibitor (etoricoxib) to conduct a series of assays, ensuring target specificity for COX-2. The differences in cell origins, disease nature, and COX target specificity help explain the divergent conclusions regarding the relationship between COX-2 and ferroptosis across studies.

The transcription factor Nrf2 was previously verified to regulate the cellular adaptive response to excessive oxidative stress and inflammation, thereby inhibiting ferroptosis in iron overload-induced liver injury.[12] Similarly, in our primary mouse hepatocyte assay, Nrf2 was downregulated in erastin-induced ferroptosis, and tBHQ stimulated Nrf2 to

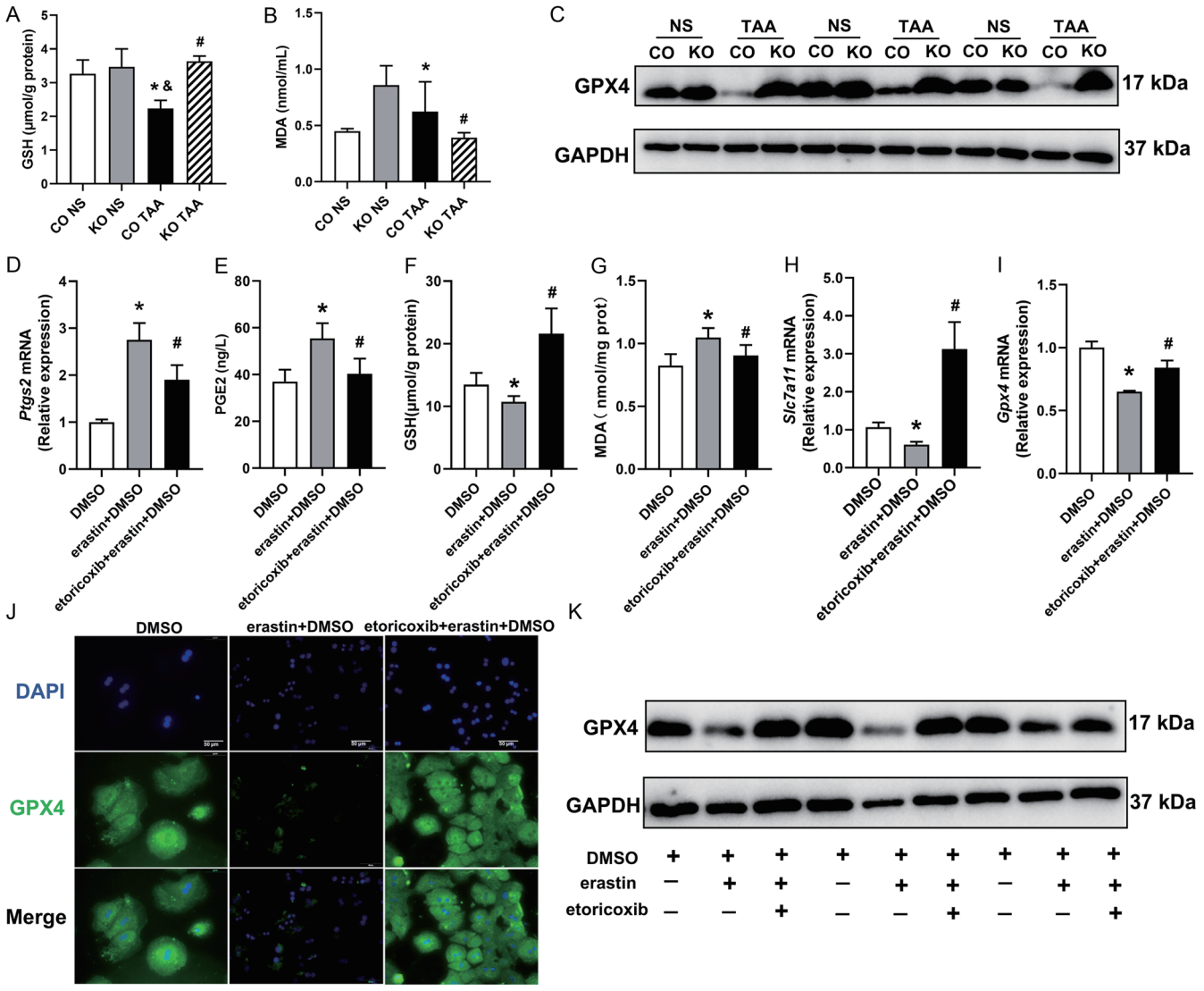

Fig. 4. Oxidative stress in mouse livers and primary mouse hepatocytes. (A, B) Concentrations of GSH and MDA in mouse livers (colorimetric assay, n = 6 for each group). (C) GPX4 expression in mouse livers (Western blot, n = 6 for each group). (D) *Ptgs2* mRNA expression level in primary mouse hepatocytes (n = 6 for each group). (E–G) Concentrations of PGE2, GSH, and MDA in primary mouse hepatocytes (colorimetric assay, n = 6 for each group). (H) *Slc7a11* mRNA expression level in primary mouse hepatocytes (n = 6 for each group). (I–K) GPX4 expression in primary mouse hepatocytes (I: qRT-PCR, n = 6 for each group; J: immunofluorescence, scale bars 50 μm, n = 6 for each group; K: Western blot, n = 4 for each group). (A–C) $p < 0.05$: **vs.* CO NS group; $^{\&}$*vs.* KO NS group; $^{\#}$*vs.* CO TAA group. (D–K) $p < 0.05$: **vs.* DMSO group; $^{\#}p < 0.05$ *vs.* erastin + DMSO group. GSH, glutathione; MDA, malondialdehyde; GPX4, glutathione peroxidase 4; CO, control; NS, normal saline; KO, knockout; TAA, thioacetamide; DMSO, dimethyl sulfoxide; +: with the reagent; -: without the reagent.

combat ferroptosis, implying that the Nrf2 signaling pathway was involved in the regulation of ferroptosis and that COX-2 affected this regulation. In combination with our *in vivo* assays, inhibition of COX-2 upregulated the Nrf2 signaling pathway to inhibit ferroptosis, ultimately impeding the progression of chronic liver diseases. This study discovers that ferroptosis is a new target of COX-2, adding to the mechanisms by which COX-2 exacerbates chronic liver diseases. Currently, several COX-2 inhibitors have been successfully developed, and selective COX-2 inhibitors are widely applied in rheumatic diseases, acute inflammation, and pain control. This study suggests that selective COX-2 inhibitors could be a potentially effective treatment for chronic liver diseases, shedding light on the potential therapeutic strategies for liver fibrosis.

Conclusions

COX-2 plays a pivotal role in ferroptosis during the progression of chronic liver disease, as it downregulates the Nrf2 signaling pathway, exacerbating ferroptosis, which is characterized by ferrous ion overload, lipid peroxidation, and excessive oxidative stress. Inhibition of COX-2 has reliable effects in alleviating liver ferroptosis and fibrosis. In future clinical practice, selective COX-2 inhibitors may serve as a potential therapeutic modality to combat liver fibrosis via ferroptosis inhibition.

Funding

This work was supported by the National Natural Science Fund of China (81700539, 82241054, and 82170625), the

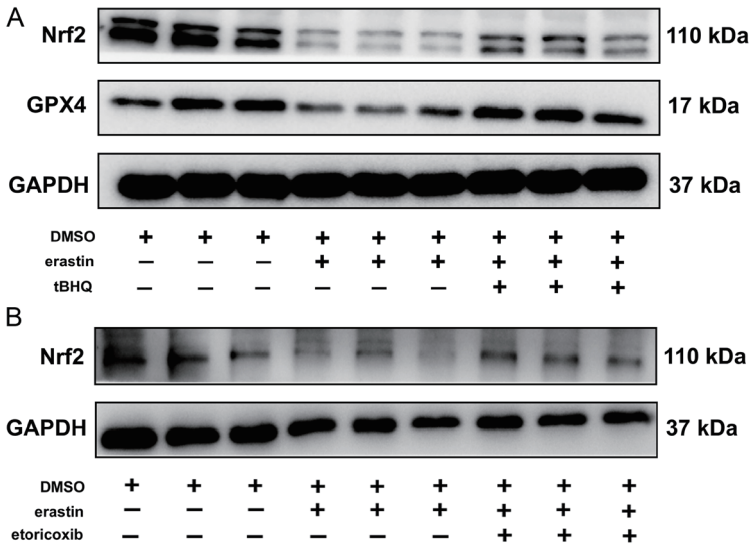

Fig. 5. Nrf2 signaling pathway of primary mouse hepatocytes. (A, B) Nrf2 and GPX4 expressions were measured in primary mouse hepatocytes by Western blot (n = 3 for each group). $p < 0.05$: **vs.* DMSO group; $^{\#}p < 0.05$ *vs.* erastin + DMSO group. Nrf2, nuclear factor erythroid 2-related factor 2; GPX4, glutathione peroxidase 4; DMSO, dimethyl sulfoxide; +: with the reagent; -: without the reagent.

135 Projects for Disciplines of Excellence at West China Hospital, Sichuan University (ZYGD23029), and the Sichuan Science and Technology Program (2024NSFSC0641).

Conflict of interest

The authors have no conflict of interests related to this publication.

Author contributions

Study concept and design (HT, JHG, CWT), acquisition of data (ZY, YT, CZ), analysis of data (ZY, YT, TL), drafting of the manuscript (ZY, YT, HT), and material support and study supervision (HT, CWT, JHG). All authors have approved the final version and publication of the manuscript.

Ethical statement

All experimental protocols were approved by the Animal Use and Nursing Committee of West China Hospital, Sichuan University (Approval No. 2017005A). All animals received human care.

Data sharing statement

All data are available from the corresponding author upon reasonable request.

References

[1] Ginès P, Krag A, Abraldes JG, Solà E, Fabrellas N, Kamath PS. Liver cirrhosis. Lancet 2021;398(10308):1359–1376. doi:10.1016/S0140-6736(21)01374-X, PMID:34543610.
[2] Aizawa S, Brar G, Tsukamoto H. Cell Death and Liver Disease. Gut Liver 2020;14(1):20–29. doi:10.5009/gnl18486, PMID:30917630.
[3] Li J, Cao F, Yin HL, Huang ZJ, Lin ZT, Mao N, *et al*. Ferroptosis: past, present and future. Cell Death Dis 2020;11(2):88. doi:10.1038/s41419-020-2298-2, PMID:32015325.
[4] Capelletti MM, Manceau H, Puy H, Peoc'h K. Ferroptosis in Liver Diseases: An Overview. Int J Mol Sci 2020;21(14):4908. doi:10.3390/ijms21144908, PMID:32664576.
[5] Yang H, Xuefeng Y, Shandong W, Jianhua X. COX-2 in liver fibrosis. Clin Chim Acta 2020;506:196–203. doi:10.1016/j.cca.2020.03.024, PMID:32184095.
[6] Li X, Mazaleuskaya LL, Ballantyne LL, Meng H, FitzGerald GA, Funk CD. Genomic and lipidomic analyses differentiate the compensatory roles of two COX isoforms during systemic inflammation in mice. J Lipid Res 2018;59(1):102–112. doi:10.1194/jlr.M080028, PMID:29180443.
[7] Chun KS, Kim EH, Kim DH, Song NY, Kim W, Na HK, *et al*. Targeting cyclooxygenase-2 for chemoprevention of inflammation-associated intestinal carcinogenesis: An update. Biochem Pharmacol 2024;228:116259. doi:10.1016/j.bcp.2024.116259, PMID:38705538.
[8] Dannenberg AJ, Altorki NK, Boyle JO, Dang C, Howe LR, Weksler BB, *et al*. Cyclo-oxygenase 2: a pharmacological target for the prevention of cancer. Lancet Oncol 2001;2(9):544–551. doi:10.1016/S1470-2045(01)00488-0, PMID:11905709.
[9] Su W, Tai Y, Tang SH, Ye YT, Zhao C, Gao JH, *et al*. Celecoxib attenuates hepatocyte apoptosis by inhibiting endoplasmic reticulum stress in thioacetamide-induced cirrhotic rats. World J Gastroenterol 2020;26(28):4094–4107. doi:10.3748/wjg.v26.i28.4094, PMID:32821072.
[10] Tai Y, Zhao C, Zhang L, Tang S, Jia X, Tong H, *et al*. Celecoxib reduces hepatic vascular resistance in portal hypertension by amelioration of endothelial oxidative stress. J Cell Mol Med 2021;25(22):10389–10402. doi:10.1111/jcmm.16968, PMID:34609050.
[11] Gao JH, Wen SL, Yang WJ, Lu YY, Tong H, Huang ZY, *et al*. Celecoxib ameliorates portal hypertension of the cirrhotic rats through the dual inhibitory effects on the intrahepatic fibrosis and angiogenesis. PLoS One 2013;8(7):e69309. doi:10.1371/journal.pone.0069309, PMID:23922700.
[12] Wu A, Feng B, Yu J, Yan L, Che L, Zhuo Y, *et al*. Fibroblast growth factor 21 attenuates iron overload-induced liver injury and fibrosis by inhibiting ferroptosis. Redox Biol 2021;46:102131. doi:10.1016/j.redox.2021.102131, PMID:34530349.
[13] Sun X, Ou Z, Chen R, Niu X, Chen D, Kang R, *et al*. Activation of the p62-Keap1-NRF2 pathway protects against ferroptosis in hepatocellular carcinoma cells. Hepatology 2016;63(1):173–184. doi:10.1002/hep.28251, PMID:26403645.
[14] Yamamoto M, Kensler TW, Motohashi H. The KEAP1-NRF2 System: a Thiol-Based Sensor-Effector Apparatus for Maintaining Redox Homeostasis. Physiol Rev 2018;98(3):1169–1203. doi:10.1152/physrev.00023.2017, PMID:29717933.
[15] Lan T, Tai Y, Zhao C, Xiao Y, Yang Z, Zhang L, *et al*. Atypical cholangiocytes derived from hepatocyte-cholangiocyte transdifferentiation mediated by COX-2: a kind of misguided liver regeneration. Inflamm Regen 2023;43(1):37. doi:10.1186/s41232-023-00284-4, PMID:37452426.
[16] Ezhilarasan D. Molecular mechanisms in thioacetamide-induced acute and chronic liver injury models. Environ Toxicol Pharmacol 2023;99:104093. doi:10.1016/j.etap.2023.104093, PMID:36870405.
[17] Lyu H, Wang H, Li L, Zhu J, Chen F, Chen Y, *et al*. Hepatocyte-specific deficiency of Nrf2 exacerbates carbon tetrachloride-induced liver fibrosis via aggravated hepatocyte injury and subsequent inflammatory and fibrogenic responses. Free Radic Biol Med 2020;150:136–147. doi:10.1016/j.freeradbiomed.2020.02.015, PMID:32112813.
[18] Zhou J, Zhang H, Zhong K, Tao L, Lin Y, Xie G, *et al*. N6-methyladenosine facilitates mitochondrial fusion of colorectal cancer cells via induction of GSH synthesis and stabilization of OPA1 mRNA. Natl Sci Rev 2024;11(3):nwae039. doi:10.1093/nsr/nwae039, PMID:38549713.
[19] Zhang L, Tai Y, Zhao C, Ma X, Tang S, Tong H, *et al*. Inhibition of cyclooxygenase-2 enhanced intestinal epithelial homeostasis via suppressing

β-catenin signalling pathway in experimental liver fibrosis. J Cell Mol Med 2021;25(16):7993–8005. doi:10.1111/jcmm.16730, PMID:34145945.
[20] Li J, Xue C, Ling X, Xie Y, Pavan D, Chen H, *et al*. A Novel Rat Model of Cardiac Donation After Circulatory Death Combined With Normothermic ex situ Heart Perfusion. Front Cardiovasc Med 2021;8:639701. doi:10.3389/fcvm.2021.639701, PMID:34368241.
[21] Hwang B, Kwon MG, Cho MJ, Lee NK, Lee J, Lee JW, *et al*. Hepatic PTP4A1 ameliorates high-fat diet-induced hepatosteatosis and hyperglycemia by the activation of the CREBH/FGF21 axis. Theranostics 2023;13(3):1076–1090. doi:10.7150/thno.79434, PMID:36793871.
[22] Xuan Q, Hu C, Yu D, Wang L, Zhou Y, Zhao X, *et al*. Development of a High Coverage Pseudotargeted Lipidomics Method Based on Ultra-High Performance Liquid Chromatography-Mass Spectrometry. Anal Chem 2018;90(12):7608–7616. doi:10.1021/acs.analchem.8b01331, PMID:29807422.
[23] Nemeth E, Tuttle MS, Powelson J, Vaughn MB, Donovan A, Ward DM, *et al*. Hepcidin regulates cellular iron efflux by binding to ferroportin and inducing its internalization. Science 2004;306(5704):2090–2093. doi:10.1126/science.1104742, PMID:15514116.
[24] Liang D, Minikes AM, Jiang X. Ferroptosis at the intersection of lipid metabolism and cellular signaling. Mol Cell 2022;82(12):2215–2227. doi:10.1016/j.molcel.2022.03.022, PMID:35390277.
[25] Kagan VE, Mao G, Qu F, Angeli JP, Doll S, Croix CS, *et al*. Oxidized arachidonic and adrenic PEs navigate cells to ferroptosis. Nat Chem Biol 2017;13(1):81–90. doi:10.1038/nchembio.2238, PMID:27842066.
[26] Tsurusaki S, Tsuchiya Y, Koumura T, Nakasone M, Sakamoto T, Matsuoka M, *et al*. Hepatic ferroptosis plays an important role as the trigger for initiating inflammation in nonalcoholic steatohepatitis. Cell Death Dis 2019;10(6):449. doi:10.1038/s41419-019-1678-y, PMID:31209199.
[27] Chen X, Li J, Kang R, Klionsky DJ, Tang D. Ferroptosis: machinery and regulation. Autophagy 2021;17(9):2054–2081. doi:10.1080/15548627.2020.1810918, PMID:32804006.
[28] Zheng Y, Zhao T, Wang J, Jiang R, Huang J, Li W, *et al*. Curcumol alleviates liver fibrosis through inducing autophagy and ferroptosis in hepatic stellate cells. FASEB J 2022;36(12):e22665. doi:10.1096/fj.202200933RR, PMID:36398583.
[29] Yu Y, Jiang L, Wang H, Shen Z, Cheng Q, Zhang P, *et al*. Hepatic transferrin plays a role in systemic iron homeostasis and liver ferroptosis. Blood 2020;136(6):726–739. doi:10.1182/blood.2019002907, PMID:32374849.
[30] Su W, Gao W, Zhang R, Wang Q, Li L, Bu Q, *et al*. TAK1 deficiency promotes liver injury and tumorigenesis via ferroptosis and macrophage cGAS-STING signalling. JHEP Rep 2023;5(5):100695. doi:10.1016/j.jhepr.2023.100695, PMID:36968217.
[31] Godoy P, Hewitt NJ, Albrecht U, Andersen ME, Ansari N, Bhattacharya S, *et al*. Recent advances in 2D and 3D in vitro systems using primary hepatocytes, alternative hepatocyte sources and non-parenchymal liver cells and their use in investigating mechanisms of hepatotoxicity, cell signaling and ADME. Arch Toxicol 2013;87(8):1315–1530. doi:10.1007/s00204-013-1078-5, PMID:23974980.
[32] Wen SL, Gao JH, Yang WJ, Lu YY, Tong H, Huang ZY, *et al*. Celecoxib attenuates hepatic cirrhosis through inhibition of epithelial-to-mesenchymal transition of hepatocytes. J Gastroenterol Hepatol 2014;29(11):1932–1942. doi:10.1111/jgh.12641, PMID:24909904.
[33] Liu Y, Zhou L, Lv C, Liu L, Miao S, Xu Y, *et al*. PGE2 pathway mediates oxidative stress-induced ferroptosis in renal tubular epithelial cells. FEBS J 2023;290(2):533–549. doi:10.1111/febs.16609, PMID:36031392.
[34] Liu J, Zhou Y, Xie C, Li C, Ma L, Zhang Y. Anti-Ferroptotic Effects of bone Marrow Mesenchymal Stem Cell-Derived Extracellular Vesicles Loaded with Ferrostatin-1 in Cerebral ischemia-reperfusion Injury Associate with the GPX4/COX-2 Axis. Neurochem Res 2023;48(2):502–518. doi:10.1007/s11064-022-03770-2, PMID:36322371.
[35] Xu Y, Liu Y, Li K, Yuan D, Yang S, Zhou L, *et al*. COX-2/PGE2 Pathway Inhibits the Ferroptosis Induced by Cerebral Ischemia Reperfusion. Mol Neurobiol 2022;59(3):1619–1631. doi:10.1007/s12035-021-02706-1, PMID:35013936.
[36] Yang WS, SriRamaratnam R, Welsch ME, Shimada K, Skouta R, Viswanathan VS, *et al*. Regulation of ferroptotic cancer cell death by GPX4. Cell 2014;156(1-2):317–331. doi:10.1016/j.cell.2013.12.010, PMID:24439385.